

# $^{99m}\text{Tc}$ -Exametazime as a Breast Tumor–Seeking Agent: Comparison with $^{99m}\text{Tc}$ -Sestamibi

Brigitte Wilczek, MD<sup>1</sup>; Leif Svensson, PhD<sup>2</sup>; Rimma Danielsson, MD, PhD<sup>1</sup>; Fuat Celebiouglu, MD<sup>3</sup>; Stig A. Larsson, PhD<sup>4</sup>; and Hans Jacobsson, MD, PhD<sup>5</sup>

<sup>1</sup>Department of Radiology, Karolinska University Hospital, Huddinge, Sweden; <sup>2</sup>Department of Hospital Physics, Karolinska University Hospital, Huddinge, Sweden; <sup>3</sup>Department of Surgery, Karolinska University Hospital, Huddinge, Sweden; <sup>4</sup>Department of Hospital Physics, Karolinska University Hospital, Solna, Sweden; and <sup>5</sup>Department of Radiology, Karolinska University Hospital, Solna, Sweden

$^{99m}\text{Tc}$ -Sestamibi is commonly used for mammoscintigraphy. Occasional uptake of  $^{99m}\text{Tc}$ -exametazime in various tumors has been described. In this study, an intraindividual comparison of these 2 radiopharmaceuticals for mammoscintigraphy was made. **Methods:** A kinetic study (30 min) in the lateral prone view of 20 breast tumors ( $\geq 1$  cm) in 20 women was conducted with  $^{99m}\text{Tc}$ -exametazime. Thereafter, 21 breast tumors ( $\geq 1$  cm) in 21 women were examined with both agents (2 patients were included in both groups) under identical conditions (interval, 2–7 d). In the latter group, the tumor-to-background breast activity ratio and the tumor uptake normalized to the administered activity (cps/MBq) at 10 min after injection were calculated and compared for both agents. **Results:** All tumors (43 tumors in 39 patients) were visualized with  $^{99m}\text{Tc}$ -exametazime. There was also one instance of false-positive uptake using this agent. The uptake phase lasted  $\sim 10$  min. Thereafter, the activity was practically stable.  $^{99m}\text{Tc}$ -Sestamibi failed to depict 4 tumors. On the group level, the tracers did not differ in tumor-to-background activity ratio or normalized tumor uptake. Intraindividual agreement in tumor-to-background ratios between the tracers was moderate (intraclass correlation coefficient = 0.49). **Conclusion:** Uptake of  $^{99m}\text{Tc}$ -exametazime in breast tumors  $\geq 1$  cm seems to be comparable with that of  $^{99m}\text{Tc}$ -sestamibi at a group level. The specificity is unknown. There is a restricted intraindividual agreement between the tracers, confirming different uptake mechanisms. This may open up possibilities for assessing different tumor characteristics in vivo, especially since the uptake of both agents is based on mechanisms believed to be involved in resistance to antineoplastic drugs.

**Key Words:** breast cancer; chemotherapy resistance; mammoscintigraphy;  $^{99m}\text{Tc}$ -exametazime;  $^{99m}\text{Tc}$ -sestamibi

J Nucl Med 2004; 45:2040–2044

The diagnosis of breast cancer is based on physical examination supported by mammography and fine-needle aspiration cytology or core biopsy. The increasing use of MRI and, especially, ultrasonography has improved diag-

nistic accuracy, but there is still a need for additional diagnostic methods. Scintigraphic evaluation of unclear breast masses has confirmed the value of mammoscintigraphy as a complementary examination for this purpose.

Several radiopharmaceuticals have been studied as tumor-seeking agents in breast cancer, and varying accuracy has been reported. Single-photon emitters include  $^{99m}\text{Tc}$ -diethylenetriaminepentaacetic acid,  $^{99m}\text{Tc}$ -pertechnetate,  $^{67}\text{Ga}$ -gallium citrate,  $^{201}\text{Tl}$ -thallium chloride,  $^{111}\text{In}$ -pentetreotide,  $^{99m}\text{Tc}$ (V)-dimercaptosuccinic acid,  $^{99m}\text{Tc}$ -methylene diphosphate,  $^{99m}\text{Tc}$ -tetrafosmin, and various  $^{99m}\text{Tc}$ -labeled antibodies (1–3). A commonly used agent for this purpose is  $^{99m}\text{Tc}$ -sestamibi (Cardiolite; Du Pont Ltd.), and several studies have confirmed its value in depicting breast tumors (4–6).

$^{99m}\text{Tc}$ -Exametazime (Ceretek; Amersham International plc) is commonly used for investigation of regional cerebral blood flow. Several reports have described occasional uptake in head and neck tumors, lung tumors, soft-tissue sarcoma, thyroid carcinoma, renal cell cancer, and hepatocellular carcinoma (7–13). Uptake by human breast tumor cell lines has also been reported (14). The purpose of this study was to explore whether  $^{99m}\text{Tc}$ -exametazime is suitable for depicting breast cancer. The uptake kinetics in breast cancer were first studied in one group of patients. Thereafter, an intraindividual comparison between uptake of  $^{99m}\text{Tc}$ -exametazime and uptake of  $^{99m}\text{Tc}$ -sestamibi was made in another patient group.

## MATERIALS AND METHODS

### Patients and Radiopharmaceuticals

Two groups of consecutive women with a recently detected breast tumor having a diameter of  $\geq 1$  cm at mammography or ultrasonography were examined. All patients underwent surgery, and the tumors were histologically graded. The study was approved by the local ethical and radiation safety committees and by the National Medical Products Agency.

To study whether  $^{99m}\text{Tc}$ -exametazime was at all suitable as a tracer for depicting breast cancer, and to study the uptake kinetics, we used it in the mammoscintigraphic examination of 20 patients (group I; mean age, 56 y; SD,  $\pm 9$  y), each of whom was given 1,000 MBq.

Received Mar. 10, 2004; revision accepted Aug. 11, 2004.  
For correspondence or reprints contact: Brigitte Wilczek, MD, Department of Radiology, Karolinska University Hospital, SE-141 86 Huddinge, Sweden.  
E-mail: brigitte.wilczek@kus.se

In group II, comprising 21 patients (mean age, 53 y; SD,  $\pm 10$  y), uptake of  $^{99m}\text{Tc}$ -exametazime and uptake of  $^{99m}\text{Tc}$ -sestamibi were compared at separate mammoscintigraphic examinations performed in random order 2–7 d apart. Each patient was given 500 MBq of each tracer. Two of these patients were also included in group I. All patients presented clinically with 1 tumor (which we termed the main tumor). In one patient in group I, an additional tumor was discovered at scintigraphy. In 3 patients in group II, an additional tumor was discovered during the diagnostic work-up before the nuclear medicine examinations.

### Tumor Characteristics

In group I, 19 of the 20 main tumors were palpable. Ten tumors were left sided and 10 were right sided. Histopathology showed 19 ductal invasive tumors, of which 7 were associated with in situ changes. According to the Elston classification, 5 cases were grade I, 8 were grade II, 5 were grade III, and 1 was grades I and II mixed. One tumor was lobular invasive grade II.

In group II, 20 of the 21 main tumors were palpable. Ten tumors were left sided and 11 were right sided. Histopathologic examination showed 19 ductal invasive tumors, of which 11 were associated with in situ changes. According to the Elston classification, 4 cases were grade I, 1 of which was associated with a lobular cancer; 11 were grade II; and 6 were grade III, including 1 case of ductal invasive tumor and lobular cancer combined.

Table 1 shows the largest diameter of the main tumor in each patient group as assessed at preoperative mammography and at specimen radiography and histopathology after resectioning.

### Mammoscintigraphy

Lateral prone views were acquired using a dual-head  $\gamma$ -camera (Sopha DST.XL; Sopha Medical Vision/General Electric Medical Systems) equipped with low-energy ultra-high-resolution parallel-hole collimators. A  $256 \times 256$  matrix giving a pixel size of 4.5 mm<sup>2</sup> was used. A dynamic 30-min planar registration was initiated when the tracer was injected in a pedal vein.  $^{99m}\text{Tc}$ -Exametazime was administered within 30 min after preparation. Acquisition was made as 20-s frames in group I and as 10-s frames in group II.

### Data Evaluation

In group I, all frames acquired from 11 to 30 min were combined into 1 image. On this, a region of interest (ROI) was drawn

around the main tumor activity with a small margin. An identical ROI was positioned in the same breast and at approximately the same distance from the chest wall representing background activity (Fig. 1). Time–activity curves were created for each of the 2 ROIs. All curves were corrected for physical decay and normalized to the area under the curve. The curves so obtained from all patients were separately combined for the tumor region and for the background region. The initial part of the 2 curves could be fitted by the least-squares technique to a monoexponential function ( $1 - e^{-\lambda t}$ ). From these data, separate measures of uptake rate ( $\lambda$ ) and of uptake half-time ( $\ln 2/\lambda$ ) could be assessed for tumor and background tissues, respectively.

In group II, the 2 examinations in each patient were evaluated on the same occasion. All frames acquired from 11 to 30 min were combined into 1 image. On this, an ROI was drawn around the main tumor, leaving a small margin. A specially designed computer program was used to select a 4-pixel-wide background region close to the tumor region, from which an interpolated background activity was calculated (Fig. 1). In 3 patients for whom no tumor uptake could be identified at examination with  $^{99m}\text{Tc}$ -sestamibi, a tumor ROI was drawn according to findings at mammography. The quotient between the activity of the tumor ROI, corrected for interpolated background to give a net tumor uptake, and the uptake of the background region was assessed as the net tumor-to-background ratio.

### Normalized Tumor Uptake

For all examinations in group II, the net tumor uptake was normalized to the administered activity of each radiopharmaceutical, thereby giving the normalized tumor uptake (cps/administered MBq). For this step, the syringe activity was measured before and after injection for 14 examinations with  $^{99m}\text{Tc}$ -exametazime and for 17 examinations with  $^{99m}\text{Tc}$ -sestamibi. The mean residual activity of the syringe at these examinations was calculated (2.6% for  $^{99m}\text{Tc}$ -exametazime and 3.9% for  $^{99m}\text{Tc}$ -sestamibi using the same type of syringe) and used to calculate the administered activity at the examinations for which the syringe activity was measured only before the injection.

### Statistical Analysis

The Wilcoxon matched-pairs test was used to compare the 2 tracers. Agreement between the tracers was calculated using the intraclass correlation coefficient. This depends in part on the corresponding product-moment correlation but also depends on the differences between the means and SDs of the 2 sets of measurements. The intraclass correlation coefficient is a reliability coefficient calculated using variance estimates obtained through an ANOVA for repeated measures. As a general guideline, values greater than 0.75 indicate good agreement and those less than 0.75 indicate moderate to poor agreement. For most clinical measurements, the value should exceed 0.90 to ensure reasonable validity (15).

## RESULTS

### Dynamic Study (Group I)

All main tumors and 1 previously undetected contralateral tumor were visualized with  $^{99m}\text{Tc}$ -exametazime. The added time–activity curves of the main tumor and the background activity had the same configuration (Fig. 2). Both curves showed an increasing uptake during  $\sim 10$  min and a practically stable activity during the subsequent 20 min. The

**TABLE 1**  
Largest Diameter of Main Tumor at Mammography and at Specimen Radiography and Histopathology After Resectioning

Patient group	Modality	Largest diameter		
		Mean (mm)	SD (mm)	Range (mm)
I	Mammography	31	16	15–70
	Radiography*	31	17	15–75
	Histology	31	16	5–65
II	Mammography†	24	11	15–50
	Radiography	25	9	13–40
	Histology	25	11	8–52

\*Two tumors did not undergo radiography.

†One tumor was not visible at mammography.

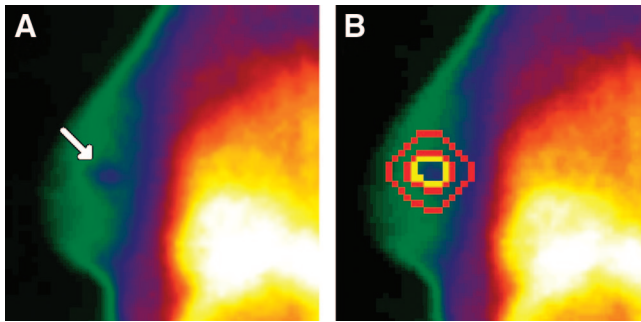


**FIGURE 1.**  $^{99m}\text{Tc}$ -exametazime mammoscintigraphy (500 MBq) of a 60-y-old woman in whom a 35-mm breast tumor was found at mammography. (A) Image showing tumor activity (arrow). (B) Same image showing ROIs used when evaluating patients of the comparative study (group II). Tumor ROI (yellow) is surrounded by 4-pixel-wide background ROI (red).

uptake half-times for the tumor and the background activity were 2.6 and 2.9 min, respectively.

### Comparative Study (Group II)

All main tumors and the 3 tumors additionally detected were visualized with  $^{99m}\text{Tc}$ -exametazime. False-positive uptake of  $^{99m}\text{Tc}$ -exametazime occurred in 1 patient, for whom complementary examination including mammography and ultrasonography showed nothing suggestive.  $^{99m}\text{Tc}$ -Sestamibi failed to depict 3 main tumors and 1 of the 3 additionally detected tumors. There were no false-positive findings with  $^{99m}\text{Tc}$ -sestamibi.

Mean ( $\pm$ SD) and median net tumor-to-background ratios for  $^{99m}\text{Tc}$ -exametazime were  $8.6 (\pm 21.2)$  and 2.3, respectively. Corresponding values for  $^{99m}\text{Tc}$ -sestamibi were  $8.7 (\pm 15.1)$  and 3.3, respectively. No difference was found between the agents ( $P = 0.82$ ) (Fig. 3).

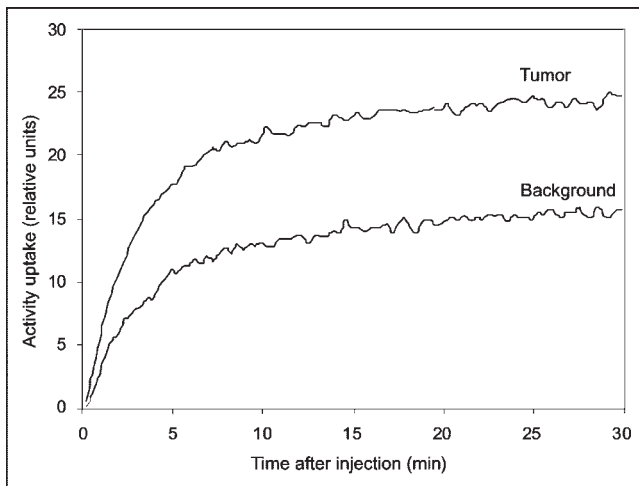


**FIGURE 2.** Time-activity curves, after correction for physical decay, of 20  $^{99m}\text{Tc}$ -exametazime examinations of breast cancer in different women. Curves show tumor uptake and uptake of a background region in ipsilateral breast. Examinations were normalized by area under curve.

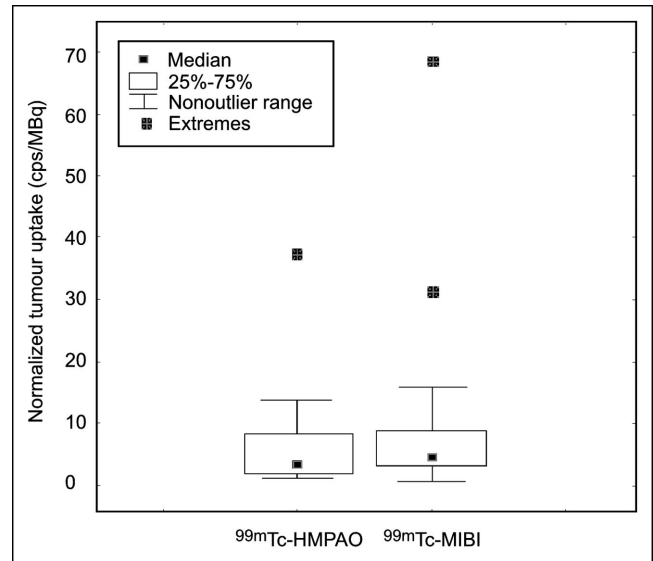


**FIGURE 3.** Box plot showing net tumor-to-background ratio of 21 breast cancers in 21 women examined with  $^{99m}\text{Tc}$ -exametazime and  $^{99m}\text{Tc}$ -sestamibi. Wilcoxon matched-pairs test showed no significant difference between the 2 tracers ( $P = 0.82$ ). HMPAO = exametazime; MIBI = sestamibi.

Mean ( $\pm$ SD) and median normalized tumor uptake at the examinations with  $^{99m}\text{Tc}$ -exametazime were  $5.9 (\pm 8.2)$  and 3.0, respectively. Corresponding values for  $^{99m}\text{Tc}$ -sestamibi were  $9.2 (\pm 15.4)$  and 3.7, respectively. No difference was found between the agents ( $P = 0.48$ ) (Fig. 4).

The net tumor uptake (%) of  $^{99m}\text{Tc}$ -sestamibi was higher than that of  $^{99m}\text{Tc}$ -exametazime in 11 patients, whereas  $^{99m}\text{Tc}$ -exametazime uptake was higher in 10 patients. The

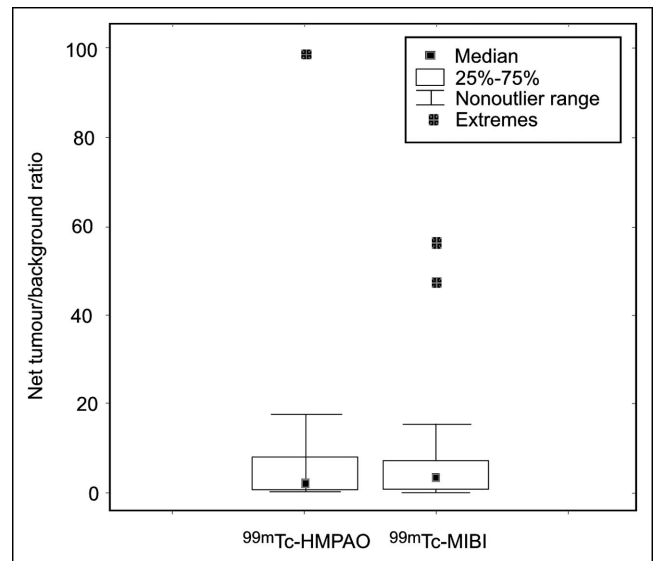


**FIGURE 4.** Box plot showing normalized uptake (cps/administered MBq) by 21 breast cancers in 21 women examined with  $^{99m}\text{Tc}$ -exametazime and  $^{99m}\text{Tc}$ -sestamibi. Wilcoxon matched-pairs test showed no significant difference between the 2 tracers ( $P = 0.48$ ). HMPAO = exametazime; MIBI = sestamibi.

ratio of net uptake between  $^{99m}\text{Tc}$ -sestamibi and  $^{99m}\text{Tc}$ -exametazime was  $<5$  in most patients. In 3 patients, however, net  $^{99m}\text{Tc}$ -sestamibi tumor uptake was more than 10 times higher than net  $^{99m}\text{Tc}$ -exametazime uptake, whereas the opposite was found in 1 patient.

The intraclass correlation reliability coefficient of net tumor-to-background ratios between the 2 radiopharmaceuticals was 0.49, indicating moderate agreement between them, as is also illustrated by Figure 5. No systematic difference was found.

## DISCUSSION

Although mammoscintigraphy is most commonly performed with  $^{99m}\text{Tc}$ -sestamibi, additional radiopharmaceuticals with different uptake mechanisms that could be used for mammoscintigraphy would strengthen its role.  $^{99m}\text{Tc}$ -Exametazime is a lipophilic agent used to examine blood flow in the brain. After crossing the blood-brain barrier, fixation is considered to depend on interaction with intracellular glutathione (16,17). Thereby, the tracer is decomposed into a hydrophilic species with a low backdiffusion. The intracellular content of glutathione is generally high in breast cancer (18), but like  $^{99m}\text{Tc}$ -sestamibi uptake,  $^{99m}\text{Tc}$ -exametazime uptake is not tumor specific. Tracer uptake is proportional to blood flow in transplantable mouse tumors (20) and in human lung (21) and brain (22) tumors, as it is in normal brain (19).

The dynamic study was necessary for the subsequent comparative study, since detailed data on the uptake kinetics of  $^{99m}\text{Tc}$ -exametazime in tumors are lacking (23–26). Compared with uptake by normal brain tissue, uptake by breast tumors (Fig. 2) is slower (19), but once fixed, it seems to be stable. The half-time for accumulation in normal brain tissue after intravenous injection has been reported to be on the order of 25–30 s (19), compared with 2.6 min in breast

tumor, as found in the present study. The reason for this discrepancy is unknown but may be due to differences in vascularity or heterogeneity of tissue. Our findings are similar to the uptake kinetics of  $^{99m}\text{Tc}$ -exametazime reported for rat and human breast tumor cell lines (14). This study, however, used a closed in vitro system with constant availability of the tracer, whereas in vivo the bolus of intact  $^{99m}\text{Tc}$ -exametazime in the circulation decomposes within a few minutes.

Using a planar single-photon technique, comparisons of absolute uptakes are questionable. Nevertheless, because all examinations in the comparative study (group II) were done within a short interval using the same  $\gamma$ -camera and under identical conditions, the comparison reported in Figure 4 is considered reasonable.

Because the aim of the present study was to compare uptake of  $^{99m}\text{Tc}$ -exametazime and  $^{99m}\text{Tc}$ -sestamibi in known breast tumors, conclusions about the accuracy of this detection are restricted. Nevertheless, the fact that all tumors were visualized with  $^{99m}\text{Tc}$ -exametazime (43 tumors in 39 patients) indicates a certain sensitivity for breast tumors  $\geq 1$  cm. Further, the only previous studies on  $^{99m}\text{Tc}$ -exametazime in breast cancer, both by the same research group, reported high sensitivity for breast cancer—detection of 16 of 17 tumors (25) and 23 of 23 tumors (26). In the pilot study (25), a specificity of 100% was reported; however, in the following study (26), for unknown reasons no specificity was assessed. Even so, no nodular uptake of the tracer occurred in the control group.

On the group level, tumor uptake of  $^{99m}\text{Tc}$ -exametazime versus the surrounding background activity did not differ from that of  $^{99m}\text{Tc}$ -sestamibi. This finding is in contrast to the higher uptake of  $^{99m}\text{Tc}$ -exametazime than of  $^{99m}\text{Tc}$ -sestamibi found in an experimental study on implanted VX-2 cancer in rabbits (27). The strength of the present study was the head-to-head comparison of the 2 agents. Such a comparison has not been reported previously. The intraindividual agreement between  $^{99m}\text{Tc}$ -exametazime and  $^{99m}\text{Tc}$ -sestamibi in our study was restricted with regard to the target-to-background ratio, thus confirming different uptake mechanisms. Further, the difference in net uptake between the 2 tracers indicates a different biologic behavior of the tracers.

The aim of the study was to compare the detectability of the 2 tracers in breast cancer, and the reason for the restricted agreement between the 2 tracers regarding uptake in individual tumors is unknown. Nevertheless, this discrepancy is striking and may open up a discussion on the possibility of using the agents for characterization of breast tumors. The uptake of both agents is based on mechanisms believed to be involved in resistance to antineoplastic drugs. Intracellular fixation of  $^{99m}\text{Tc}$ -exametazime is considered to be based on interaction with glutathione (16,17). A correlation exists between elevated cellular concentrations of glutathione and resistance to alkylating agents and cisplatin (28,29). These drugs may be inactivated through conjuga-

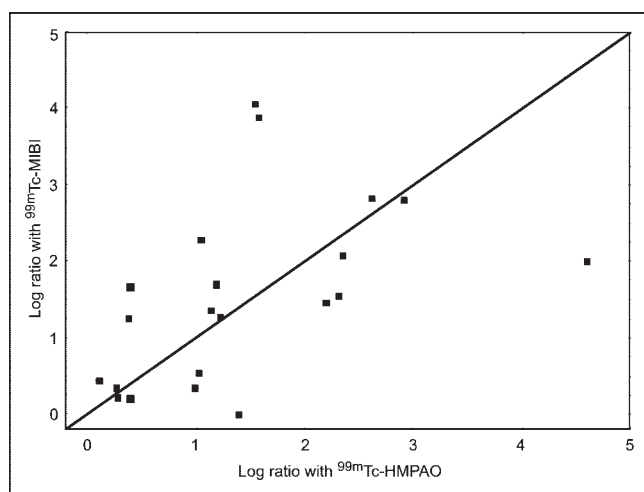


**FIGURE 5.** Scatterplot with line of equality showing relationship between log net tumor-to-background ratios at examinations with  $^{99m}\text{Tc}$ -exametazime and  $^{99m}\text{Tc}$ -sestamibi in same patients. HMPAO = exametazime; MIBI = sestamibi.



tion with intracellular glutathione by catalysis of glutathione S-transferases and thereafter extruded from the cells (30,31). Another type of drug resistance is caused by an efflux of drugs from tumor cells mediated by the adenosine triphosphate-dependent transmembrane transporter proteins P-glycoprotein and multidrug-resistance protein (32,33). The washout rate of  $^{99m}\text{Tc}$ -sestamibi from tumor cells correlates positively with the expression of these proteins (34,35). One might predict that the 2 tracers would be affected oppositely. Glutathione or its enzymes can be elevated in multidrug-resistant tumors, and thus  $^{99m}\text{Tc}$ -exametazime accumulation would be elevated and  $^{99m}\text{Tc}$ -sestamibi accumulation reduced. However, glutathione may be independent of multidrug resistance. As a further confounding factor, glutathione can also be elevated in hypoxic tumors. Testing these hypotheses would require early and late examination with  $^{99m}\text{Tc}$ -sestamibi as well as biopsy information from the tumors, with immunohistochemistry to document levels of glutathione and other nonprotein sulfhydryls, glutathione-related enzymes, and multidrug-resistance transporters. Such studies were beyond the scope of the present investigation.

## CONCLUSION

$^{99m}\text{Tc}$ -Exametazime can be used to depict breast cancer.  $^{99m}\text{Tc}$ -Sestamibi failed to reveal 3 of the main tumors and 1 additional tumor, all of which were detected by  $^{99m}\text{Tc}$ -exametazime. Consequently, the sensitivity of  $^{99m}\text{Tc}$ -exametazime for mammoscintigraphy seems to be comparable to that of  $^{99m}\text{Tc}$ -sestamibi or may even be higher. No conclusions can be reached about the specificity of  $^{99m}\text{Tc}$ -exametazime for mammoscintigraphy.

## ACKNOWLEDGMENTS

We thank Elisabeth Berg, BSc, Karolinska Institute, Sweden, for performing the statistical analysis; Jane Wigertz, Nyköping, Sweden, for revising the language; and Professor Curt Peterson, Linköping University, Sweden, for introducing us to principles of drug resistance.

## REFERENCES

- Bombardieri E, Crippa F, Maffioli L, Greco M. Nuclear medicine techniques for the study of breast cancer. *Eur J Nucl Med.* 1997;24:809–824.
- Taillefer R. The role of  $^{99m}\text{Tc}$ -sestamibi and other conventional radiopharmaceuticals in breast cancer diagnosis. *Semin Nucl Med.* 1999;29:16–40.
- Goldenberg DM, Nabi HA. Breast cancer imaging with radiolabeled antibodies. *Semin Nucl Med.* 1999;29:41–48.
- Aktolun C, Bayhan H, Kir M. Clinical experience with Tc-99m MIBI imaging in patients with malignant tumors: preliminary results and comparison with Tl-201. *Clin Nucl Med.* 1992;17:171–176.
- Khalkhali I, Mena I, Jouanne E, et al. Prone scintimammography in patients with suspicion of carcinoma of the breast. *J Am Coll Surg.* 1994;178:491–497.
- Danielsson R, Boné B, Gad A, Sylvan M, Aspelin P. Sensitivity and specificity of planar scintimammography with  $^{99m}\text{Tc}$ -sestamibi. *Acta Radiol.* 1999;40:394–399.
- Minn H, Ahonen A, Paul R. Radiation effects on uptake of  $^{99m}\text{Tc}$ -hexamethylpropylene amine oxime (HMPAO) in head and neck tumours. *Br J Cancer.* 1991;64:735–740.
- Rowell NP, Flower MA, McCready VR, Cronin B, Horwich A. The effects of single dose oral hydralazine on blood flow through human lung tumours. *Radiother Oncol.* 1990;18:283–292.

- Rowell NP, Flower MA, Cronin B, McCready VR. Quantitative single-photon emission tomography for tumour blood flow measurement in bronchial carcinoma. *Eur J Nucl Med.* 1993;20:591–599.
- Sinnott HD, Rowell NP, McCready VR, Lawrence R. Demonstration of blood flow patterns in human soft tissue sarcomas using  $^{99m}\text{Tc}$ -labelled hexamethylpropylene amineoxime. *Br J Surg.* 1990;77:454–457.
- Marienhagen J, Hohenberger W, Rodl W, Herbst M, Wolf F. Tumour imaging with  $^{99m}\text{Tc}$ -HMPAO in metastatic thyroid cancer: first results. *Nuc Compact.* 1998;19:234–237.
- Tzukamoto E, Takumara A, Sakurai Y, Saito H, Tamaki N. Tc-99m HMPAO in renal cell carcinoma metastases. *Clin Nucl Med.* 1997;22:569–570.
- Otsuka N, Fukunaga M, Morita K, et al. Accumulation of  $^{99m}\text{Tc}$ -HMPAO in photon deficient areas in bone scan of bone metastases from hepatocellular carcinoma. *Ann Nucl Med.* 1992;6:215–220.
- Ballinger JR, Duncan J, Hua HA, Ichise M. Accumulation of  $^{99m}\text{Tc}$ -HMPAO and  $^{99m}\text{Tc}$ -ECD in rodent and human breast tumor cell lines in vitro. *Ann Nucl Med.* 1997;11:95–99.
- Shrout PE, Fleiss JL. Interclass correlations: uses in assessing rater reliability. *Psychol Bull.* 1979;86:420–428.
- Neirinckx RD, Burke JF, Harrison RC, Forster AM, Andersen AR, Lassen NA. The retention mechanism of technetium-99m-HM-PAO: intracellular reaction with glutathione. *J Cereb Blood Flow Metab.* 1988;8(suppl 1):S4–S12.
- Suess E, Malessa S, Ungersböck K, et al. Technetium-99m-d,l-hexamethylpropyleneamine oxime (HMPAO) uptake and glutathione contents in brain tumors. *J Nucl Med.* 1991;32:1675–1681.
- Murray GI, Burke MD, Ewen SW. Glutathione localisation in benign and malignant human breast lesions. *Br J Cancer.* 1987;55:605–609.
- Andersen AR, Friberg HH, Schmidt JF, Hasselbalch SG. Quantitative measurements of cerebral blood flow using SPECT and [ $^{99m}\text{Tc}$ ]-d,l-HM-PAO compared to xenon-133. *J Cereb Blood Flow Metab.* 1988;8(suppl 1):S69–S81.
- Hammersley PAG, McCready VR, Babich JW, Coghlan G.  $^{99m}\text{Tc}$ -HMPAO as a tumour blood flow agent. *Eur J Nucl Med.* 1987;13:90–94.
- Rowell NP, McCready VR, Tait D, et al. Technetium-99m HMPAO and SPECT in the assessment of blood flow in human lung tumours. *Br J Cancer.* 1989;59:135–141.
- Langen K-J, Roosen N, Herzog H, et al. Investigations of brain tumours with  $^{99m}\text{Tc}$ -HMPAO SPECT. *Nucl Med Commun.* 1989;10:325–334.
- Ohnishi T, Noguchi S, Murakami N, et al. Early and delayed imaging of Tc-99m HMPAO versus Tl-201 in benign and malignant thyroid tumors: similar uptake but different retention. *Clin Nucl Med.* 1992;17:806–811.
- Suga K, Uchisako H, Honma Y, et al. The assessment of  $^{99m}\text{Tc}$ -HMPAO tumor scintigraphy using VX-2 tumors in rabbits. *Kaku Igaku.* 1991;28:1049–1056.
- Ussov WY, Scopinaro F, Popadic S, et al. Scintimammography with  $^{99m}\text{Tc}$ -HMPAO in detection of breast cancer [abstract]. *Eur J Nucl Med.* 2002;29(suppl 1):S69.
- Ussov WY, Scopinaro F, Medvedeva AA, Obradovic VB, Velichko SA, Slonimskaya EM. Single-photon detection of breast cancer using  $^{99m}\text{Tc}$ -HMPAO: kinetics of uptake and imaging of tumour [abstract]. *Eur J Nucl Med.* 2003;30(suppl 2):S289.
- Otsuka N, Mimura H, Morita K, et al. Study on tumor accumulation property of  $^{99m}\text{Tc}$ -HM-PAO and  $^{99m}\text{Tc}$ -MIBI in rabbits bearing VX-2 cancer. *Kaku Igaku.* 1995;32:199–203.
- Chuman Y, Chen ZS, Sumizawa T, et al. Characterization of the ATP-dependent LTC4 transporter in cisplatin-resistant human KB cells. *Biochem Biophys Res Commun.* 1996;226:158–165.
- Friedman HS, Colvin OM, Kaufmann SH, et al. Cyclophosphamide resistance in medulloblastoma. *Cancer Res.* 1992;52:5373–5378.
- Kepler D, Leier I, Jedlitschky G, König J. ATP-dependent transport of glutathione S-conjugates by the multidrug resistance protein MRP1 and its apical isoform MRP2. *Chem Biol Interact.* 1998;111–112:153–161.
- Barnouin K, Leier I, Jedlitschky G, et al. Multidrug resistance protein-mediated transport of chlorambucil and melphalan conjugated to glutathione. *Br J Cancer.* 1998;77:201–209.
- Broxterman HJ, Schuurhuis GJ. Transport proteins in drug resistance: detection and prognostic significance in acute myeloid leukemia. *J Intern Med.* 1997;240(suppl):S147–S151.
- Ling V. Multidrug resistance: molecular mechanisms and clinical relevance. *Cancer Chemother Pharmacol.* 1997;40(suppl):S3–S8.
- Vecchio SD, Ciarmiello A, Potena MI, et al. In vivo detection of multidrug-resistant (MDR1) phenotype by technetium-99m sestamibi scan in untreated breast cancer patients. *Eur J Nucl Med.* 1997;24:150–159.
- Kostakoğlu L, Kiratli P, Ruacan S, et al. Association of tumor washout rates and accumulation of technetium-99m-MIBI with expression of P-glycoprotein in lung cancer. *J Nucl Med.* 1999;39:228–234.